Planar force-constant models and internal strain parameter of Ge and Si

P. Molinàs-Mata and M. Cardona
Max-Planck-Institut für Festkörperforschung, Heisenbergstrasse 1, D-7000 Stuttgart 80, Federal Republic of Germany

(Received 11 September 1990; revised manuscript received 3 December 1990)

The phonon-dispersion relations of Ge and Si along [100] and [111] are accurately fitted with planar force-constant models, including a generalization that treats electronic as well as ionic degrees of freedom. Expressions for the internal strain parameter ζ as a function of the planar force constants for longitudinal phonons propagating along [111] and for transverse phonons along either [100] or [111] are derived. It is shown that these expressions lead to inconsistent values of ζ if the electronic degrees of freedom are omitted. Their inclusion restores consistency and leads to values of ζ equal to 0.577 ± 0.027 for Ge and 0.564 ± 0.030 for Si.

I. INTRODUCTION

Planar force-constant models have been successfully used to describe phonon-dispersion relations of Si, Ge, and GaAs,[1] as well as different kinds of superlattices[2-5] along high-symmetry directions of **K** space. The corresponding force constants can be obtained either by fitting experimental dispersion relations[1,6] or, theoretically, by means of total-energy band-structure calculations.[7] These constants can be used to estimate the elusive internal strain parameter ζ first introduced by Kleinman[8] to describe relative sublattice deformations under the action of uniaxial strain along [111]. This parameter plays a crucial role in the elastic and lattice dynamical properties (for an excellent review of work on ζ prior to 1981 see Ref. 9).

The planar force-constant models used so far include only interactions between atomic planes. It is well known, however, that electronic degrees of freedom can help to improve the fits to phonon dispersion relations, thus reducing the number of required parameters. Among these models we mention the shell[6] and bond-charge models.[10,11] In this paper we introduce electronic degrees of freedom into the planar force-constant models and fit the phonon dispersion relations of Ge and Si. We compare the fits with those obtained without electronic degrees of freedom and show that the fits are improved by the inclusion of the electron-electron and electron-ion force constants. In particular, excellent fits are obtained for the rather difficult TA phonon-dispersion branches.

We also derive analytic expressions for the ζ parameter as a function of the planar force constants, including electronic degrees of freedom. This is possible for longitudinal vibrations along [111] and for transverse ones along either [111] or [100]. The fitted planar force constants that include electronic degrees of freedom give values of ζ which agree with reliable theoretical values (e.g., from total-energy calculations[12,13]) and with the most recent experimental results.[14] However, without electronic degrees of freedom large discrepancies between the obtained values of ζ and the accepted ones are found. The ζ's obtained without electronic degrees of freedom from phonon data for various directions of propagation and polarization are not consistent with each other.

The planar force-constant models possess the advantage of being easier to handle than the full three-dimensional calculations (a reduction from a three-dimensional problem to a one-dimensional one is performed; the resulting 2×2 secular equations can be solved analytically). They present, however, the drawback of being obliged to fit the different dispersion curves independently, i.e., independent sets of parameters are obtained for the different directions of propagation and polarization; not surprisingly, the obtained fits are excellent.

In Sec. II we present two models of planar force constants: a simple one with only the common planar force constants to fourth nearest neighbors; and a more elaborate one that includes the electronic degrees of freedom by setting bond-charge planes midway between the ionic planes, and incorporates the three possible sorts of interactions arising from this two different plane types: ion–ion, bond-charge–bond-charge, and ion–bond-charge. The latter model, in the spirit of Weber for the three-dimensional case[10] but considering neither the Coulomb interaction nor a Keating parameter for bond-charge–bond-charge interaction, offers the advantage of fitting remarkably well the TA modes.

Not only very accurate fits are reported for this second model but the differences in the quality of the fits and the errors associated with each free parameter are summarized in Sec. III. Section III A considers the Ge case and, due to the lack of recent and faithful inelastic neutron-scattering data for silicon, a type of scaling data generation[15,16] is introduced to obtain a set of reliable data for the Si at 80 K (Sec. III B) using the best available results for Ge at 80 K.[17,18]

In Sec. IV A we discuss the determination of ζ (the internal strain parameter) by means of our model. It is clearly shown how important the electronic degrees of

freedom are in order to reproduce, within such a simple planar model, the more recent and accepted results obtained with full-energy calculations (see Sec. IV B), keeping the predicted uncertainty at a reasonable level. Finally, Sec. IV C is devoted to the discussion of the results, in particular why within our model only the internal strain parameter associated with the ions needs to be considered and no similar parameter for the bond charges can be introduced.

II. PLANAR FORCE-CONSTANT MODELS

A symmetry analysis[19] of the group of the **K** vector inside the Brillouin zone (BZ) shows that when **K** is parallel to [100] (Δ line), the phonon symmetries are $\Delta_1(A)$ (LA, nondegenerate), $\Delta_{2'}(O)$ (LO, nondegenerate), $\Delta_5(A)$ (TA twofold degenerate), and $\Delta_5(O)$ (TO twofold degenerate). At the edge of the BZ in this direction (point X), where it becomes necessary to deal with *projective* representations[20,21] due to the fact that O_h^7 is a *nonsymmorphic* space group, the $\Delta_1(A)$ and $\Delta_{2'}(O)$ modes become degenerate and their symmetry is labeled X_1. The other two sets of phonons remain doubly degenerate, being labeled X_3 (TA) and X_4 (TO).

Similar analyses can be performed for the group of the **K** vector along the [111] direction (line Λ). The number and degeneracy of the phonons are the same as along Δ. Here the symmetry assignments are $\Lambda_1(A)$ (LA), $\Lambda_1(O)$ (LO), $\Lambda_3(A)$ (TA), and $\Lambda_3(O)$ (TO). However, at the BZ boundary (the L point) no degeneracy occurs between $\Lambda_1(A)$ and $\Lambda_1(O)$. Therefore four phonon frequencies, corresponding to $L_{2'}$(LA), L_1(LO), L_3(TA), and $L_{3'}$(TO) symmetries should be considered.

Symmetry guarantees the decoupling of the 6×6 dynamical matrix into two 2×2 ones: one for the longitudinal and another (doubly degenerate) for the transverse modes. Along high symmetry directions, such as [100] or [111], there is no coupling between longitudinal and transverse modes. Consequently, the vibrations of planes perpendicular to [100] or [111], which move as rigid units, may be described as those of linear chains. This transformation of the three-dimensional dynamical problem is exact and entails the diagonalization of similar matrices for both longitudinal and transverse modes along the high symmetry lines. Although the secular equations are formally the same, different sets of force constants k_n are expected to fit the experimental data for each direction.

The first model we present involves ion-ion planar force constants $k(l,n;l',n')$, giving the restoring force

$$F(l,n) = -k(l,n;l',n')v(l',n'), \tag{1}$$

which is produced at the l plane of the n planar unit cell by a displacement of the l' plane of the n' planar unit cell . Using *Bloch's theorem*, it becomes possible to relate any plane displacement to a displacement inside the primitive planar cell

$$v(l,n) = v(l,o)e^{iKan}, \tag{2}$$

where K is the magnitude of the **K** vector along the symmetry direction under study and a corresponds to the projection along this high symmetry direction of the shortest out-of-plane lattice vector. We allow the interactions between planes to reach the fourth nearest neighbors for both [100] and [111] directions [see Figs. 1(a) and 2(a)]. This approach can be achieved with six constants for both the [111] tranverse and longitudinal modes and for the [100] transverse ones, due to the fact that $k_n=k_{-n}$ if n is even. Only three constants are needed (up to third nearest neighbors) for the [100] longitudinal modes because $k_n=k_{-n}$ for any n.

The dynamical matrix[22] (D) for **K** along a high symmetry direction and a given phonon polarization (longitudinal or transverse) has the matrix elements

$$(D)_{11} = (D)_{22} = M\omega^2 - 2\sum_{j=1}^{N/2-\sigma} k_{2j}\,[1-\cos(Kaj)] - \sum_{j=0}^{N/2+\sigma-1} (k_{2j+1} + k_{-(2j+1)}) \tag{3}$$

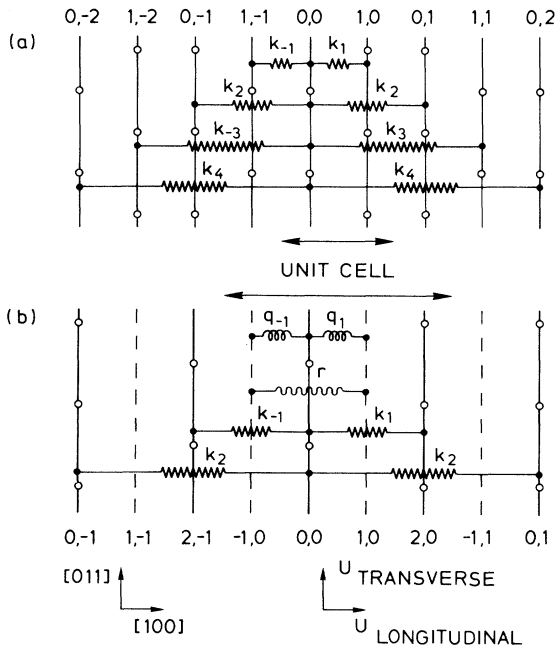

FIG. 1. Planar interactions included in the present models (see text) for the **K** vector along [100]. In (a) only interactions between *atomic* planes up to the fourth neighbors are considered; in (b) interactions between *ionic* planes up to second neighbors, interactions between *bond-charge planes* (BCP) and the nearest *ionic* planes, and between nearest BCP are introduced. For the longitudinal case the number of parameters is reduced due to symmetry ($k_1=k_{-1}$, $k_3=k_{-3}$, and $q_1=q_{-1}$). The planes are labeled with two indices: (l,n). The first one describes the plane inside the planar primitive unit cell we deal with and the second one corresponds to the planar primitive unit cell. (b) has the horizontal scale expanded by a factor of 2 with respect to (a), although the planar primitive unit cell is identical.

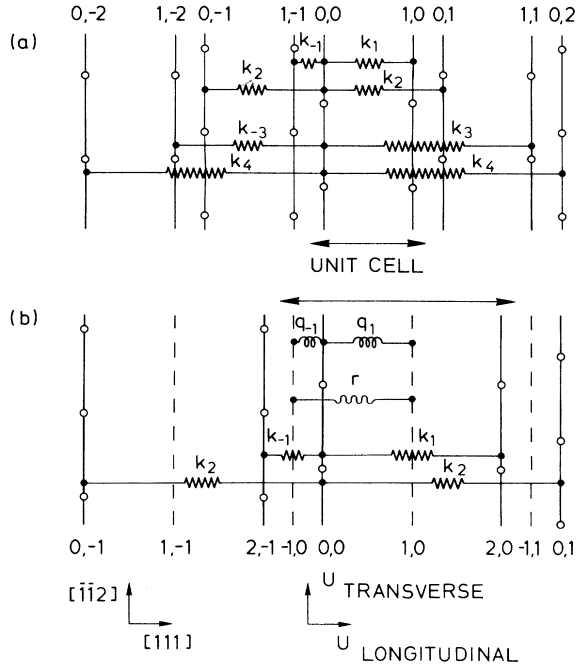

FIG. 2. Planar interactions of the presented models (see text) for the **K** vector along [111]. The description is the same that of Fig. 1, however, no simplification occurs in the longitudinal case on account of symmetry.

and

$$(D)_{12} = (D)^*_{21} = \sum_{j=-N/2-\sigma}^{N/2+\sigma-1} k_{2j+1} e^{iKaj}, \tag{4}$$

where N represents the farthest nearest-neighbor plane we consider, and $\sigma = \frac{1}{4}[1-(-1)^N]$. N different planar force constants appear in the [100] longitudinal case, while for either [111] L, [100] T, or [100] T, $(3N/2)+\sigma$ constants appear due to the symmetry properties already mentioned. Diagonalization of D provides the eigenvalues and eigenvectors of the corresponding acoustic and optical vibrational modes.

For three-dimensional lattice dynamical models it has been shown[10] that the introduction of electronic degrees of freedom (bond charges) considerably reduces the number of parameters required to fit the experimental phonon dispersion curves, in particular the TA branches. In the same spirit, we introduce here planes of near zero mass midway between atomic (*ionic*) planes, perpendicular to the propagation direction, and call them *bond-charge* planes (BCP). Such modeling of the electronic degrees of freedom does not allow the BCP to behave independently of the ionic lattice because not only the BCP-BCP interactions are considered but also those between the BCP and ionic planes. The BCP contain the bond charges of Weber's model, therefore our model is closer to it than to conventional shell models. Thus it is more adequate than the latter in representing covalent bonding effects. The bond charges connected by the BCP have site symmetry D_{3d}. In three-dimensional bond-charge models electrostatic long-range lattice sums have to be performed (however, Weber showed that for Ge a purely short-range bond-charge model, without electrostatic long-range interactions, gives almost the same results as that with long-range forces[11]). The inclusion of long-range interactions in planar models is not necessary since the field of a periodically charged plane decays exponentially normal to it, corresponding to the fact that the field of an uniformly charged plane is independent of distance.

As shown in Figs. 1(b) and 2(b), our BCP model includes three kinds of interactions: ion-ion planes up to second nearest neighbors (k), ion planes-BCP (q), and BCP-BCP (r), the latter two up to first nearest neighbors. For both the [111] longitudinal and transverse modes and for the [100] transverse ones this requires six parameters: k_1, k_{-1}, k_2, q_1, q_{-1}, and r; because of the S_4 axis only three parameters are needed for the [100] longitudinal modes (up to first neighbors): k_1, q_1, and r. Each primitive cell contains four planes: two ionic and two BCP. Their displacements are $v_{-1,n}$, $v_{1,n}$, and $v_{0,n}$, $v_{2,n}$, respectively. The use of Bloch's theorem transforms the lattice dynamical problem (for whichever range of the ion-ion plane interaction) into the following 4×4 eigenvalues problem

$$\left[M\omega^2 - \left(q_1 + q_{-1} + 2\sum_{j=1}^{N/2-\sigma} k_{2j}(1-\cos Kaj) + \sum_{j=0}^{N/2+\sigma-1}\left(k_{2j+1} + k_{-(2j+1)}\right)\right)\right] v_{0,0}$$
$$+ \sum_{j=-N/2-\sigma}^{N/2+\sigma-1} k_{2j+1} e^{iKaj} v_{2,0} + q_1 v_{1,0} + q_{-1} v_{-1,0} = 0, \tag{5}$$

$$\left[M\omega^2 - \left(q_1 + q_{-1} + 2\sum_{j=1}^{N/2-\sigma} k_{2j}(1-\cos Kaj) + \sum_{j=0}^{N/2+\sigma-1}\left(k_{2j+1} + k_{-(2j+1)}\right)\right)\right] v_{2,0}$$
$$+ \sum_{j=-N/2-\sigma}^{N/2+\sigma-1} k_{2j+1} e^{-iKaj} v_{0,0} + q_1 v_{1,0} + q_{-1} v_{-1,0} e^{iKa} = 0, \tag{6}$$

$$q_1 v_{0,0} + q_1 v_{2,0} + \left[m\omega^2 - 2(q_1 + r)\right] v_{1,0} + r\left(1 + e^{+iKa}\right) v_{-1,0} = 0, \tag{7}$$

and

$$q_{-1} v_{0,0} + q_{-1} e^{-iKa} v_{2,0} + \left[m\omega^2 - 2(q_{-1} + r)\right] v_{-1,0} + r\left(1 + e^{-iKa}\right) v_{1,0} = 0, \tag{8}$$

where M is the atomic mass, m is *formally* the mass of the BCP, and both σ and N are defined as in Eqs. (3) and (4). The substitution of Eqs. (7) and (8) into (5) and (6), i.e., the *decimation* of the electronic degrees of freedom, results in *renormalized* force constants for the ionic motion which depend on the frequency. This dependence disappears when the limit $m \rightarrow 0$ is taken; this implies that the BCP do not stay fixed but move adiabatically. The phonon frequencies are again found by solving a 2×2 eigenvalues problem with renormalized force constants which depend on **K** but not on ω, i.e., a quadratic equation.

III. FITS TO THE PHONON-DISPERSION RELATIONS MEASURED ALONG [100] AND [111] DIRECTIONS

In order to adjust the free parameters of both models described in Sec. II, inelastic neutron-scattering data have been fitted using computer codes[23] (see Table I). The function to be minimized is χ_R^2, defined as

$$\chi_R^2 = \frac{1}{N_d - N_p} \sum_{t=1}^{T} \frac{\left(\nu_{\mathrm{expt}_t} - \nu_{\mathrm{theor}_t}\right)^2}{\left(er\nu_{\mathrm{expt}_t}\right)^2} \tag{9}$$

where T is the number of fitted experimental frequencies (typically around 20), ν_{expt_t} and ν_{theor_t} are the experimental and theoretical frequencies ($\nu = \omega/2\pi$) for the t point of the BZ in a high symmetry direction, $er\nu_{\mathrm{expt}_t}$ is the experimental error associated with ν_{expt_t} (errors should be assumed to be normally distributed to give full statistical meaning to χ_R^2), N_d is the number of experimental points, and N_p is the number of fitting parameters. The error given in Table I for each free parameter represents the square root of the corresponding diagonal term of the covariance matrix (calculated by inverting the second derivative matrix evaluated numerically by the finite difference method[23]), multiplied by a numerical factor which depends on the desired confidence interval [$\sqrt{10.65}$ (or $\sqrt{6.25}$) for the 90% confidence interval taken for all the cases, using six (or three) free parameters, respectively].[26] Table II displays the values of χ_R^2 [see Eq. (9)] for the best fits obtained in each case.

Lack of information concerning the estimate of errors in Refs. 17 and 18 restricts the use of χ_R^2 as a meaningful statistical indicator of the quality of the fits.[27] We thus do not discuss whether each fit is statistically representative or not. Assuming that errors have been properly estimated, a value of χ_R^2 close to $\simeq 1$ (the exact value depends on the number of degrees of freedom[28]) should be taken as the most probable one if χ_R^2 is evaluated for new experimental points and the same fitted parameters. A moderate decrease of χ_R^2 can be considered as indicative of improvement in modeling the lattice dynamics. However, the best indication of a model improvement arises from the values of ζ obtained (see Sec. IV). They are rather close to each other regardless of the different polarization branches and compare well with the most reliable information available from other sources.

A. Germanium

Nilsson and Nelin's data[17,18] for Ge longitudinal phonons along the [100] (Δ line) at 80 K can be fitted equally well with both models, whereby only three parameters (Table I) are required to obtain very high quality fits to the data (see Fig. 3 and Table II). This results from the fact that both LA and LO curves are rather smooth and that there is an extra symmetry-imposed constraint for this polarization, namely the degeneracy of both acoustic and optical modes at the X point. In spite of the relatively large χ_R^2 value for this case, the fit

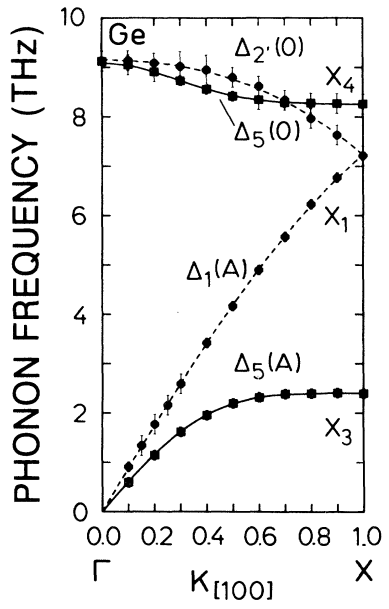

FIG. 3. Phonon dispersion relations $\nu(\mathbf{K})$ of germanium for the *longitudinal* (dashed lines) and *transverse* (solid lines) modes along [100] determined by fitting the experimental data (Refs. 17 and 18) with the three and six parameters of the BCP model (Table I), for the longitudinal and transverse polarization, respectively. This fit is almost identical for the planar *ionic* force-constant model using only the three and six corresponding constants of Table I and, for this reason, it has not been plotted. The error bars are *ten times* larger than the experimental ones.

TABLE I. Fitted and calculated planar force constants for Ge and Si. Errors are given in parentheses. The values in brackets are characterized by an error larger than 100%. This error arises from the insufficient information which is carried by very smooth longitudinal mode dispersion curves when too many parameters in the BCP model are taken to fit the experimental data. All constants are expressed in S.I. (N/m).

	100 L			100 T		111 L	111 T
				Ge			
k_1[a]	99.73(0.50)			164.31(0.64)		108.84(5.6)	−7.6(1.6)
k_{-1}	99.73(0.50)			1.7(1.6)		86.3(7.0)	179.3(1.5)
k_2	12.37(0.41)			−4.85(0.44)		8.52(0.86)	−2.1(0.7)
k_3	{0.06(0.28)}			21.8(1.8)		{1.5(6.9)}	5.28(0.93)
k_{-3}	{0.06(0.28)}			8.52(0.79)		{1.2(5.5)}	20.6(1.8)
k_4				−1.62(0.40)		{0.2(0.5)}	−1.0(0.5)
q_1[b]	3246(22)			1.061(0.001)		−6.8(2.1)	59.8(3.1)
q_{-1}	3246(22)			121.0(3.8)		41.(23.)	8.93(0.15)
r	50.1(1.5)			−1.044(0.001)		11.9(5.5)	−7.19(0.11)
k_1	−1523(11)			156.3(0.62)		107.4(1.9)	−9.5(1.8)
k_{-1}	−1523(11)			−20.6(2.5)		74(13)	173.3(1.5)
k_2				2.90(0.45)		9.3(2.0)	3.35(0.74)
k_1	105.0[c]			169.5[c]		114.2[c]	10.1[c]
k_{-1}	105.0			20.3		90.0	189.9
k_2	8.3			−8.6		5.4	−4.8
k_3	{0.6}			3.5		2.0	4.4
k_{-3}	{0.6}			9.4		2.9	2.4
k_4	{−1.4}			−2.9		−2.0	{−2.1}
k_5				0.7			
k_{-5}				2.3			
k_6				{−1.5}			
				Si			
k_1[a]	116.71(0.67)			185.32(0.86)		124.6(6.2)	−9.3(2.2)
k_{-1}	116.71(0.67)			5.3(2.9)		99.1(7.7)	204.8(1.9)
k_2	15.02(0.55)			−4.80(0.59)		9.8(1.2)	−2.19(0.94)
k_3	{0.10(0.37)}			23.4(3.1)		{1.7(7.6)}	6.4(1.3)
k_{-3}	{0.10(0.37)}			9.51(0.98)		{1.3(5.8)}	24.7(2.4)
k_4				−2.06(0.51)		{0.21(0.63)}	−1.13(0.67)
q_1[b]	3246(28)			1.052(0.001)		−7.8(2.8)	74.6(7.1)
q_{-1}	3246(28)			130.3(4.3)		48(30)	10.33(0.27)
r	61.0(1.5)			−1.036(0.001)		13.7(7.9)	−8.43(0.18)
k_1	−1506(14)			175.71(0.76)		123.0(2.5)	−12.6(4.3)
k_{-1}	−1506(14)			−18.1(2.9)		85(18)	197.7(1.9)
k_2				3.99(0.53)		10.7(2.8)	4.5(1.0)
k_1	94.2[d]	111.3[e]	149.0[d]	181.9[e]	183.0[f]	121.3[g]	18.6[g]
k_{-1}	94.2	111.3	29.0	32.5	33.0	101.7	204.9
k_2	16.3	13.0	−4.0	−6.93	−8.0	2.8	−4.9
k_3	0.8	1.28	1.0	0.62	1.0	0.1	4.5
k_{-3}	0.8	1.28	8.0	8.84	8.0	6.1	0.7
k_4		0.25		−1.10		0.1	−0.7
k_5						0.0	0.6
k_{-5}						0.4	0.1
k_6						0.0	−0.1

[a] Present work without BCP.
[b] Present work with BCP.
[c] Reference 24, local-density function (LDF) *ab initio* calculation.
[d] Reference 7, LDF *ab initio* calculation.
[e] Reference 6, fit to shell and bond charge model fit.
[f] Reference 1, planar force-constant fit.
[g] Reference 25, fit to bond-charge model of Ref. 10. This contains also k's for Ge.

TABLE II. Values of the minimized χ_R^2 function [see Eq.(9)], for germanium and silicon along Δ and Λ lines.

100 L	100 T	111 L	111 T
	germanium		
3.45[a]	0.96[a]	1.98[a]	0.84[a]
3.46[b]	0.66[b]	1.61[b]	0.30[b]
	silicon		
2.87[a]	2.65[a]	1.48[a]	0.72[a]
2.88[b]	0.77[b]	1.20[b]	0.33[b]

[a] Present work, fit without BCP.
[b] Present work, fit with BCP.

should be considered fairly good because basically only three constants are used. The χ_R^2's value obtained with BCP for [100] L modes is essentially the same and no particular advantage of the BCP model appears in this case; the fitted curves are indistinguishable for both models and only one has been plotted in Fig. 3. The fit with the BCP model in the [100] T case improves χ_R^2 by 30% (see Table II), even though the difference in the fits cannot be appreciated in Fig. 3. Comparing with the longitudinal [100] fit, the χ_R^2 is reduced provided that six parameters are fitted instead of three.

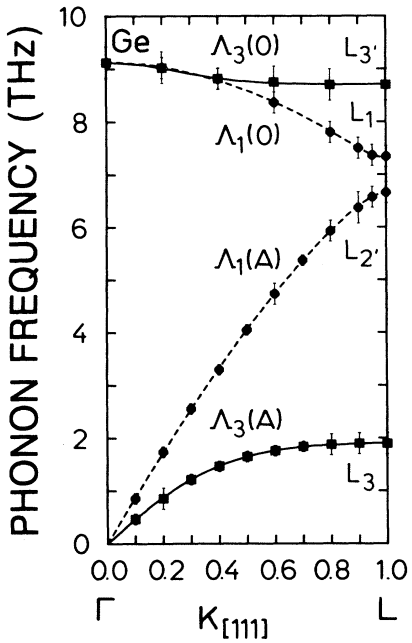

FIG. 4. Phonon-dispersion relations $\nu(\mathbf{K})$ of germanium for the *longitudinal* and *transverse* modes along [111] determined by fitting the experimental data (Refs. 17 and 18) with the six parameters of the BCP model (Table I). Dashed and solid lines correspond to longitudinal and transverse modes, respectively. This fit is almost identical for the planar *ionic* force-constant model using the six constants of Table I and, for this reason, it has not been plotted. The error bars have been drawn *ten times* larger than the experimental ones.

In the [111] cases six parameters are also introduced for either longitudinal or transverse modes, although the longitudinal ones can be fairly well fitted taking into account only first- and second-neighbor ionic planar interactions (see Table I). In Fig. 4 the best fits for longitudinal and transverse modes along the Λ line, obtained with BCP (see Table II), are plotted. Better fits (lower χ_R^2) are obtained for the BCP model, especially for the [111] transverse modes. The improvement of χ_R^2 produced by the inclusion of the BCP is nearly a factor of 3 for the [111] T case.

In order to provide a feeling for this general improvement, the difference between the fitted curve for the first model and for the second one (with BCP) has been plotted versus the **K** vector along Δ for the transverse case in Fig. 5. These differences are of the order of 0.3% or smaller for all of our fits.

Reasonably good agreement is found between some *ab initio* calculations[24,25] for the planar force constants and our fitted results with only ionic planar interaction for the longitudinal polarization. Since the dispersion curves calculated by Kunc and Gomez Dacosta[24] do not reproduce the characteristic flattening of the TA phonons, also their force constants and our fitted values without BCP show significant differences (see Table I). Some ionic force constants for nearer neighbors are found to be smaller than some for farther neighbors, thus raising the question of convergence and whether interactions with farther planes should not be included. However, a larger number of free parameters makes the model useless since not enough experimental information is available for their determination. The introduction of the BCP seems to avoid this disturbing increase of the absolute value of the planar ionic force constants with interplanar distance.

B. Silicon

Due to the fact that the available inelastic neutron-scattering data at 296 K for silicon[29] are not as ac-

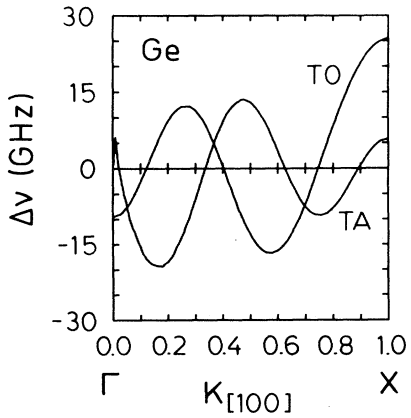

FIG. 5. Difference between the two different fitted phonon dispersion curves (with and without BCP) for the transverse polarization along the [100] direction.

curate as Nilsson and Nelin's results for germanium at 80 K (Refs. 17 and 18) interpolation and scaling method has been developed based on the similarities between the frequency dispersion curves of silicon and germanium. The hypothesis that silicon and germanium have dimensionless dispersion curves of rather similar shape in reduced units has been discussed by introducing the simplest possible combination of the atomic mass m, the lattice constant a, and the electron charge e, which has the dimensions of a frequency[15,16]

$$\sqrt{e^2/ma^3}. \tag{10}$$

The frequencies for different crystals are thus reduced to dimensionless values $\bar{\nu}$, where

$$\bar{\nu} = \sqrt{(ma^3/e^2)}\nu, \tag{11}$$

and the $\mathbf{K}$'s to their dimensionless counterparts $\tilde{\mathbf{K}}=(a/2\pi)\mathbf{K}$.

These substitutions allow us, in principle, to obtain the phonon dispersion curves for silicon by scaling the germanium results.[17,18] When comparing these predictions with the few and not too precise data available for silicon, however, small but significant differences are found. Hence we have introduced four different factors in order to center the generated data for each phonon branch around Dolling's room-temperature results[29] scaled by a temperature coefficient (1.006) so as to represent data at 80 K. The additional factors, which increase slightly and not uniformly the frequencies predicted by the simple scaling of Eq.(11) are, for the [100] direction, 1.023 (LA), 1.018 (LO), and 1.001 (TO), and for the [111] direction, 1.008 (LA), 1.007 (LO), 1.055 (TA), and 1.007 (TO). More accurate data exist for the transverse acoustic branches (TA) for Si along the [100] direction at room temperature.[16] We scaled them by the temperature factor (1.006) to obtain transverse acoustic data at 80 K. This nonuniform scaling procedure should lead to a larger and more accurate set of experimental data compared to Dolling's results,[29] although centered around them for each branch. These phonon frequencies are rather close to those predicted by scaling the germanium ones, although some minor but significant deviations from the uniform scaling are found. Note that a uniform scaling from Ge data will produce identical ζ values for Si as for Ge on account of the invariance of ζ with respect to an uniform scaling of all force constants [see Eqs. (16)–(18)].

IV. INTERNAL STRAIN PARAMETER AND PLANAR FORCE CONSTANTS

When a macroscopic stress is applied to a solid with more than one atom per primitive cell, the possibility of relative displacements of these atoms (internal strains) arises.[30–32] In the case of the diamond lattice the only possible internal strain is a displacement of the two sublattices by a vector δ. Well known symmetry conditions[30–32] reduce such possibilities. For instance, a pure longitudinal internal strain is only possible for a [111] uniaxial stress. Only for directions of applied uniaxial stress within a (001) plane, between [100] and [110], pure perpendicular internal strain (along [001]) is obtained; it is zero for [100] and maximum for [110].[30] For all other cases internal strains with both parallel and perpendicular components to the applied uniaxial stress are found. Internal strains appear also with the macroscopic *shear strains* which accompany long-wavelength TA phonons along either [100] or [111]. In the diamond structure the internal strain is related to the macroscopic strain through only one parameter labeled ζ.[8]

A. Theoretical approach

It is possible to determine the value of the internal strain parameter ζ using the planar force-constant results which fit the experimental phonon-dispersion curves.[1] Essentially, an affine transformation, which produces a parallel or perpendicular displacement of each plane whose magnitude is proportional to the distance to a fixed plane (plane 0 in Figs. 6–8), can be decomposed into

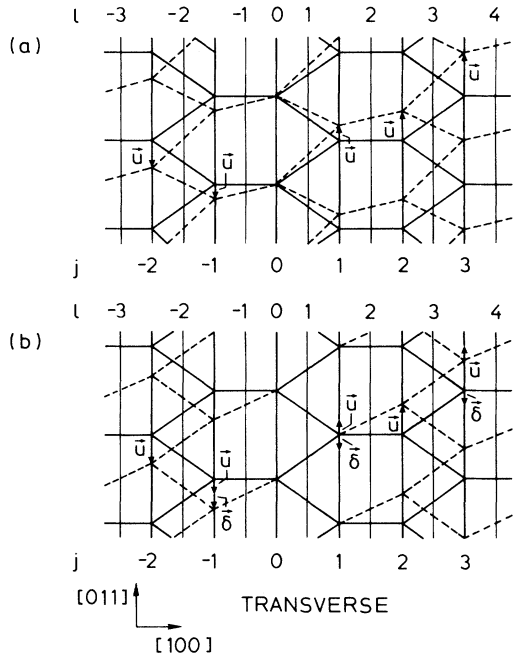

FIG. 6. Planar projections of the diamond lattice when an affine transformation which moves the (100) planes with a perpendicular displacement proportional to the distance to a generic plane labeled 0 is performed (see text). (a) corresponds to the case $\zeta=0$: the lattice transforms *everywhere* following the affine transformation pattern and (b) reproduces the behavior for $\zeta=1$; the internal strain *neutralizes* totally the affine transformation within each unit cell, i.e., the *bonds* between the ionic planes: . . .,(−2,1),(0,1),(2,3),. . . remain *unstrained.* The ionic planes are labeled with j and the BCP with l.

a *shear strain* $\overleftrightarrow{\epsilon}_S$, a rotation $\overleftrightarrow{\epsilon}_R$, and a *hydrostatic* compression or dilatation $\overleftrightarrow{\epsilon}_C$ ($\epsilon_{Cij}=\epsilon_C\delta_{ij}$). The expression for the total strain tensor is $\overleftrightarrow{\epsilon}=\overleftrightarrow{\epsilon}_S+\overleftrightarrow{\epsilon}_R+\overleftrightarrow{\epsilon}_C$.[33] Such an affine transformation can be constructed easily by looking for the expected displacement of the parallel planes with respect to an arbitrarily fixed plane. The relation between such a transformation and a phonon is provided by taking, for example, for the [100] transverse case, the phonon displacement components $u_x \sim 0$, $u_y \sim e^{iK_x x}$, and $u_z \sim e^{iK_x x}$ in the limit $K_x \simeq 0$. In this case, [100] transverse, we obtain

$$\overleftrightarrow{\epsilon}=\overleftrightarrow{\epsilon}_S+\overleftrightarrow{\epsilon}_R=\frac{2\sqrt{2}}{a}\begin{pmatrix}0&0&0\\1&0&0\\1&0&0\end{pmatrix}$$
$$=\frac{\sqrt{2}}{a}\begin{pmatrix}0&1&1\\1&0&0\\1&0&0\end{pmatrix}+\frac{\sqrt{2}}{a}\begin{pmatrix}0&\bar{1}&\bar{1}\\1&0&0\\1&0&0\end{pmatrix}, \tag{12}$$

where a is the lattice constant and a particular normalization of the phonon amplitude has been taken. Due to internal strains, not all the ionic positions will remain at the positions given by an affine transformation. We consider only the internal displacement δ of one sublattice with respect to the other and linear[34] in the components of the shear matrix $\overleftrightarrow{\epsilon}_S$. The diamond symmetry of the lattice dictates[35,36] that

$$\delta_i=-\frac{a}{4}\zeta\,|\eta_{ijk}|\,\epsilon_{jk}, \tag{13}$$

where ζ is the internal strain parameter, η_{ijk} the Levi-Civita tensor, and ϵ_{ij} the components of the strain tensor. Using Eq. (13) and the strain matrix for a given phonon we find the relation between $|\delta|$ and ζ. In the example of Eq. (12),

$$|\delta|=-\zeta. \tag{14}$$

Imposing the static equilibrium condition at the mentioned arbitrary plane, around which we produce the affine transformation, provides an equation for ζ as a function of the planar force constants (see Ref.1 for the cases [100] transverse and [111] longitudinal with planar ion-ion force constants only). Including the electronic planar force constants we find for the [100] transverse phonons (see Fig. 6)

$$\sum_{j\,\mathrm{odd}}(j+|\delta|)\,k_j+\sum_l\left(l-\frac{\mathrm{sgn}(l)}{2}+\frac{|\delta|}{2}\right)q_l=0, \tag{15}$$

which can be solved for $|\delta|$ and related to ζ with Eq. (14), obtaining

$$\zeta_{[100]T}=-|\delta|=\frac{\sum_{j\,\mathrm{odd}}jk_j+\sum_l lq_l-\frac{1}{2}\sum_l\mathrm{sgn}(l)q_l}{\sum_{j\,\mathrm{odd}}k_j+\frac{1}{2}\sum_l q_l}. \tag{16}$$

The constants k_j and q_l are commonly labeled with inte-

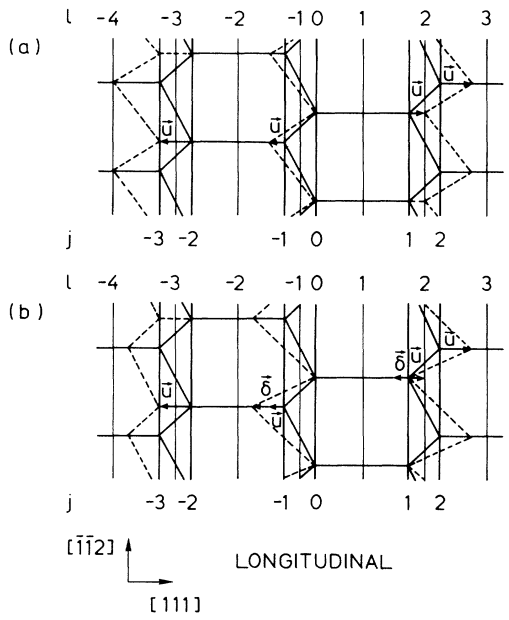

FIG. 7. Planar projections of the diamond lattice for (a) $\zeta=0$ and (b) $\zeta=1$ when an affine transformation is performed moving longitudinally along the (111) planes (see Fig. 6 caption and text).

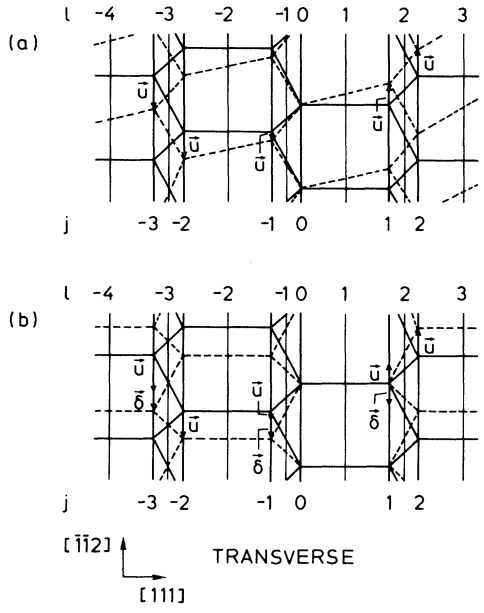

FIG. 8. Planar projections of the diamond lattice for (a) $\zeta=0$ and (b) $\zeta=1$ when an affine transformation is performed moving along $[\bar{1}\bar{1}2]$ the (111) planes (see Fig. 6 caption and text).

ger numbers corresponding to the plane number on the right (positive label) and on the left (negative label except if $k_j=k_{-j}$, $q_l=q_{-l}$) as can be seen in Fig. 6. The term sgn(l) represents the sign of l.

Similar expressions are found for the [111] direction and the longitudinal (Fig. 7) and transverse (Fig. 8) modes, respectively:

$$\zeta_{[111]\mathrm{L}}=\frac{\sum_{j\,\mathrm{odd}}(\frac{1}{2}+j)k_j+\sum_l\{l+\frac{1}{2}[\frac{1}{2}-\mathrm{sgn}(l)]\}q_l}{\sum_{j\,\mathrm{odd}}k_j+\frac{1}{2}\sum_l q_l} \tag{17}$$

and

$$\zeta_{[111]\mathrm{T}}=\frac{\sum_{j\,\mathrm{odd}}[-1-2j]\,k_j+\sum_l[\mathrm{sgn}(l)-\frac{1}{2}-2l]q_l}{\sum_{j\,\mathrm{odd}}k_j+\frac{1}{2}\sum_l q_l}. \tag{18}$$

Note that the expression on the right-hand side of Eq. (18) is equivalent to that for Eq. (17) multiplied by -2. The values of ζ calculated with both expressions should, however, be the same within the errors of the planar force constants used. The errors in the ζ's were calculated using the error propagation expressions,[28] which involve the diagonal and nondiagonal covariance matrix elements so as to take into account correlation between the fitting parameters. In Figs. 6–8 limiting behaviors of the internal strain for [100] transverse, [111] longitudinal, and [111] transverse, respectively, are depicted. They correspond to $\zeta=0$ in (a) and $\zeta=1$ in (b). $\zeta=0$ implies that all the atoms and bond charges sit at the positions induced by the macroscopic strain giving the affine transformation. In the opposite case, $\zeta=1$, the bond lengths behave rigidly because the internal strain applied to the second sublattice neutralizes the affine transformation. Only the ions of the first sublattice are then localized at the places predicted by the affine transformation (this should always happen due to the translational invariance of the crystal).

B. Results

In Table III the values of ζ obtained with our fitted planar force constants are compared with those obtained with other models, *ab initio* theoretical calculations, and experimental results. Only for the estimate from longitudinal [111] phonons does the introduction of BCP not change ζ within the error bars. Estimates from transverse phonons lead to a very different ζ, depending on whether the BCP electronic degrees of freedom are included or not. On the whole, the values obtained with the BCP model are consistent for the three phonon dispersion curves within the estimated errors, in spite of a possible systematic discrepancy involving lower ζ for the longitudinal [111] parameters. This and the fact that much larger discrepancies appear if no BCP are included (only k_i force constants) lend considerable support to the BCP model. Good agreement of the BCP model with the total-energy calculations of ζ also exists.[12,13] Intriguing agreement also appears between the revised x-ray measurements,[14] especially with the BCP internal strain parameter obtained from longitudinal polarization

TABLE III. Fitted, theoretical, and experimental values of the internal strain parameter ζ for germanium and silicon.

100 T	111 L	111 T
	germanium	
1.031 ± 0.036[a]	0.619 ± 0.049[a]	1.356 ± 0.093[a]
0.594 ± 0.012[b]	0.548 ± 0.039[b]	0.588 ± 0.030[b]
0.600[c]	0.603[c]	
	0.44±0.02[d] 0.51[e,f] 0.52[g] 0.53[h] 0.546[i]	
	0.54±0.04[j] 0.64±0.04[k] 0.76±0.04[l]	
	silicon	
0.992 ± 0.55[a]	0.618 ± 0.055[a]	1.373 ± 0.110[a]
0.579 ± 0.013[b]	0.547 ± 0.043[b]	0.566 ± 0.044[b]
0.53[m] 0.57[n]		
	0.38[o] 0.45[e] 0.50[g] 0.5±0.1[p] 0.51[q]	
	0.53[d,f] 0.533[r] 0.54[s] 0.546[t] 0.55[h]	
	0.557[i] 0.58[u] 0.61[v]	
	0.52±0.02[w] 0.54±0.04[j] 0.62/0.65*±0.04[k]	
	0.72±0.04[x] 0.71/0.75*±0.07[l] 0.74±0.04[y]	

[a] Present work, fit without BCP.
[b] Present work, fit with BCP.
[c] Reference 24, local-density function *ab initio* calculation.
[d] Reference 37, local-density function pseudopotential calculation.
[e] Reference 38, deformation potential calculation.
[f] Reference 39, *ab initio* pseudopotencial calculation.
[g] Reference 11, adiabatic bond-charge calculation.
[h] Reference 40, Keating model fit.
[i] Reference 41, Keating and Coulomb interaction fit.
[j] Reference 14, x-ray diffraction, review of Ref.9.
[k] Reference 30, x-ray diffraction. Asterisk denotes value revised in Ref.9.
[l] Reference 42, x-ray diffraction. Asterisk denotes value revised in Ref.9.
[m] Reference 1, using data from Ref.7.
[n] Reference 1, planar force-constant fit.
[o] Reference 43, *ab initio* pseudopotential calculation.
[p] Reference 44, deformation potential calculation.
[q] Reference 13, linear muffin-tin orbital fast full-potential calculation.
[r] Reference 45, valence-force-field model fit.
[s] Reference 6, shell and bond-charge model fit, ion ζ.
[t] Reference 45, using data from Ref.46.
[u] Reference 6, shell and bond-charge model fit, shell ζ.
[v] Reference 12, linear combination of atomic orbitals calculation.
[w] Reference 47, estimated value from eigenvectors phase functions ϕ, comparing with bond-charge model and valence-force-field model fits.
[x] Reference 9, x-ray diffraction.
[y] Reference 48, x-ray diffraction.

along [111] (i.e., uniaxial stress along [111] used in the determination of ζ).

C. Discussion

The site symmetry of charges placed at the center of the bonds (D_{3d}, with a center of inversion, the same as that of O atoms in cubic SiO_2, i.e., cristobalite) rules out additional internal strain parameters associated with the electronic degrees of freedom: both in Weber's model[10] and in our BCP model, the atomic displacements of the bond charges, odd under inversion, cannot couple to the even strains. This is not the case in models with electronic shells centered on the ions. In this case one can define a ζ associated with the ions and another describing the center of the electronic shell. The former would be measured with neutron diffraction while the latter would contribute, together with the former, to x-ray measurements. It has been shown in Ref. 6, by fitting a shell and bond-charge model, that both ζ's are rather close for Si [ζ(ion)=0.54, ζ(electronic shell)=0.58].

V. CONCLUSIONS

The internal strain parameters ζ for Ge and Si have been determined by using two different planar force-constant models: one including electronic degrees of freedom (BCP) and the other without them. Although both models produce nearly perfect fits to experimental data (see Table II), the introduction of the BCP in order to simulate the electronic degrees of freedom midway between the ionic planes leads to slightly better fits for all the cases except for the longitudinal phonon dispersion curves along Δ. Our BCP model implies the equivalence of the internal strain parameter ζ for electrons and ions and provides consistent values of ζ for different propagation and polarization directions of the fitted dispersion curves. Thus reliable values of ζ around 0.57 for both Ge and Si are determined, in agreement with most existing theoretical estimates.

The planar force constants obtained here can be used advantageously for the investigation of the lattice dynamics of Ge- and Si-based superlattices[49] with either [100] or [111] growth axes, in particular, of the effects of electronic degrees of freedom. The internal strain parameter is rather important for calculations of elastic constants,[41] phonon-phonon interaction constants (anharmonicity),[45,46] and electron-phonon constants.[38,44,50] Nevertheless direct experimental determinations of ζ (so far only through x-ray diffraction) yield values ranging from 0.54 to 0.76 for germanium and silicon. The last reported value is $\zeta = 0.54 \pm 0.04$.[14] These values were obtained from nominally larger ones by noticing an increase in uniaxial strain near the sample surface and appropriately correcting for it.[14] While this increase was determined with x-ray scattering techniques, it remains obscure how such increase (and not the opposite, i.e., strain relaxation) can build up. In view of the unsolved experimental situation one has to look for the guidance of theoretical calculations, in particular those based on minimization of total energies obtained from *ab initio* band structures (only available for Si).[12,13] A number of other, more indirectly calculated values are also listed in Table III; the calculated values of ζ cluster around 0.51 in Ge and 0.52 in Si.

As already mentioned, consistency between the three values of ζ obtained from planar force constants for phonons propagating along [100] and [111] is only obtained if electronic degrees of freedom (BCP) are included. The average value of ζ found in this manner is 0.577 ± 0.027 for Ge and 0.564 ± 0.030 for Si. These values agree with most of the theoretical estimates given in Table III and rule out reported experimental data higher than 0.7. They are reasonably accurate and reliable enough to be used as a data base in calculations for which they are required, until better experimental data become available. The latter could result from neutron-diffraction experiments in which the whole stressed sample contributes and the surface problem is thus avoided.

The differences in the BCP-model values of ζ for the various directions of phonon propagation and polarization, while marginal within the error bars, could be related to the poor convergence of Eqs. (16)–(18) in which the force constants appear multiplied by j, the neighborhood order of the plane under consideration.

ACKNOWLEDGMENTS

Valuable discussions with M. I. Alonso, K. Kunc, G. Martínez, W. Kress, and R. Migoni are gratefully acknowledged. Thanks are also due to G.C. La Rocca for enlightening discussions about symmetry properties and error analysis. It is a pleasure to thank C.Grein for his careful reading of a draft of this paper. P.M.M. acknowledges the Directorate-General for Science, Research and Development (European Community) for financial support.

[1] M. Cardona, K. Kunc, and R.M. Martin, Solid State Commun. 44, 1205 (1982).
[2] A. Fasolino and E. Molinari, J. Phys. (Paris) Colloq. 48, C5-569 (1987).
[3] A. Fasolino, E. Molinari, and J. C. Maan, Superlatt. Microstruct. 3, 117 (1987).
[4] E. A. Monte, G. F. A. van de Walle, D. J. Gravesteijn, A. A. van Gorkum, and W. J. O. Teesselink, Semicond. Sci. Technol. 4, 889 (1989).
[5] A. Fasolino, E. Molinari, and K. Kunc, Phys. Rev. B 41, 8302 (1990).
[6] M. T. Labrot, A. P. Mayer, and R. K. Wehner, *Phonons 89*,

edited by S. Hunklinger, W. Ludwig, and G. Weiss (World Scientific, Singapore, 1990), p.181.
[7]M. T. Yin and M.L. Cohen, Phys. Rev. B **25**, 4317 (1982).
[8]L. Kleinman, Phys. Rev. **128**, 2614 (1962).
[9]C. S. G. Cousins, J. Phys. C **15**, 1857 (1982).
[10]W. Weber, Phys. Rev. Lett. **33**, 371 (1974).
[11]W. Weber, Phys. Rev. B **15**, 4789 (1977).
[12]B. N. Harmon, W. Weber, and D. R. Hamann, Phys. Rev. B **25**, 1109 (1982).
[13]M. Methfessel, C. O. Rodríguez, and O.K. Andersen, Phys. Rev. B **40**, 2009 (1989).
[14]C. S. G. Cousins, L. Gerward, J. Staun Olsen, B. Selsmark, B. J. Sheldon, and G. E. Webster, J. Phys. C **20**, 29 (1987).
[15]T. I. Kucher, Fiz. Tverd. Tela (Leningrad) **4**, 2385 (1962) [Sov. Phys.—Solid State **4**, 1747 (1963)].
[16]G. Nilsson and G. Nelin, Phys. Rev. B **6**, 3777 (1972).
[17]G. Nilsson and G. Nelin, Phys. Rev. B **3**, 364 (1971).
[18]G. Nelin and G. Nilsson, Phys. Rev. B **5**, 3151 (1972).
[19]M. Lax, *Symmetry Principles in Solid State and Molecular Physics* (Wiley, New York, 1974), p. 363.
[20]G. I. Bir and G. L. Pikus, *Symmetry and Deformation Effects in Semiconductors* (Wiley, New York, 1974), p. 88.
[21]F. Bassani and G. Pastori Parravicini, *Electronic States and Optical Transitions in Solids* (Pergamon, New York, 1975), p. 48.
[22]A. A. Maradudin, E. W. Montroll, G. H. Weiss, and I. P. Ipatova, *Theory of Lattice Dynamics in the Harmonic Approximation* (Academic, New York, 1971).
[23]F. James and M. Roos, Comput. Phys. Commun. **10**, 343 (1975).
[24]K. Kunc and P. Gomes Dacosta, Phys. Rev. B **32**, 2010 (1985).
[25]A.Fleszar and R.Resta, Phys. Rev. B **34**, 7140 (1986).
[26]W.T.Eadie *et al.*, *Statistical Methods in Experimental Physics* (North-Holland, Amsterdam, 1971).
[27]W.H.Press, B.P.Flannery, S.A.Teukolsky, and W.T. Vetterling, *Numerical Recipes* (Cambridge University Press, Cambridge, England, 1986).
[28]P.R.Bevington, *Data Reduction and Error Analysis for the Physical Sciences* (McGraw-Hill, New York, 1969).
[29]G. Dolling, *Inelastic Scattering of Neutrons in Solids and Liquids* (International Atomic Energy Agency, Vienna, 1963), Vol. II, p. 37.
[30]A. Segmüller and H. R. Neyer, Phys. Kondens. Mater. **4**, 63 (1965).
[31]H. Freese and W. Döring, Z. Phys. B **34**, 135 (1979).
[32]E. Anastassakis and M. Cardona, Phys. Status Solidi B **104**, 589 (1981).
[33]L. A. Shuvalov, *Modern Crystallography IV* (Springer, Heidelberg, 1988), p. 57.
[34]M. Born and K. Huang, *Dynamic Theory of Crystal Lattices* (Clarendon, Oxford, 1956), p.135.
[35]J. L. Birman, Phys. Rev. **111**, 1510 (1958).
[36]J. F. Nye, *Physical Properties of Crystals* (Clarendon, Oxford, 1960), p.124.
[37]O. H. Nielsen and R. M. Martin, Phys. Rev. Lett. **50**, 697 (1985); Phys. Rev. B **32**, 3792 (1985).
[38]L. Brey, N. E. Christensen, and M. Cardona, Phys. Rev. B **36**, 2638 (1987).
[39]A. Fukumoto, Phys. Rev. B **42**, 7462 (1990).
[40]P. N. Keating, Phys. Rev. **145**, 637 (1966).
[41]R. M. Martin, Phys. Rev. B **1**, 4005 (1970).
[42]A. Segmüller, Phys. Kondens. Mater. **3**, 18 (1964).
[43]Zong-Quan Gu, Ming-Fu Li, Jian-Qing Wang, and Bing-Sing Wang, Phys. Rev. B **41**, 8333 (1990).
[44]N. E. Christensen, Solid State Commun. **50**, 177 (1984).
[45]E. Anastassakis, A. Cantarero, and M. Cardona, Phys. Rev. B **41**, 7529 (1990).
[46]D. Vanderbilt, S. H. Taole, and S.Narasimhan, Phys. Rev. B **40**, 5657 (1989).
[47]D. Strauch, A. P. Mayer, and B.Dorner, Z. Phys. B **78**, 405 (1990).
[48]H. D'Amour, W. Denner, H. Schulz, and M. Cardona, J. Appl. Cryst. **15**, 148 (1982).
[49]M. I. Alonso, M. Cardona, and G. Kanellis, Solid State Commun. **69**, 479 (1989); **70**, i (1989).
[50]A.Blacha, H.Presting, and M.Cardona, Phys. Status Solidi B **12**, 11 (1974).